

Low Phase Noise Oscillators including some Detailed Designs

Jeremy Everard

Department of Electronics,
University of York,
Heslington, York, YO10 5DD, UK
jkae@ohm.york.ac.uk

Abstract— This paper describes a linear theory for the design of low phase noise oscillators. A set of design rules are then developed for fixed frequency and tunable oscillators. The paper then describes a detailed design example which is one of the laboratory classes offered to final (4th year) MEng undergraduate degree students and to Masters level students at the University of York, UK.

I. INTRODUCTION

The oscillator in communication and measurement systems, defines the reference signal onto which modulation is coded and later demodulated. The flicker and phase noise in such oscillators are central in setting the ultimate systems performance limits of modern communications, radar and timing systems. These oscillators are therefore required to be of the highest quality for the particular application as they provide the reference for data modulation and demodulation.

This paper describes a linear theory for low phase noise oscillators. This theory is used to develop a set of design rules which typically enable oscillators to be designed with performance within ~ 0 to 1dB of the theoretical minimum performance.

II. PHASE NOISE THEORY

It is important to develop a simple model to calculate and predict the noise performance of an oscillator. Leeson [1] demonstrated an equation which gives useful information about the phase noise but the optimum conditions for minimum noise are not clear. Parker [2] demonstrated an optimum condition for a modified version of Leeson's equation. It is useful, however, to develop a simple model, from first principles, which enables an accurate and clearly understood equation to be derived.

A suitable model is shown in figure 1 [3][4]. This consists of an amplifier with two inputs which are added together. These represent the same input but are separated to enable one to be used to model the noise input and the other for feedback. The resonator is represented as an LCR circuit where any impedance transformation is achieved by varying

the component values. This circuit, through positive feedback, operates as a Q multiplication filter but also contains the additional constraint that the AM noise is suppressed in the limiting process. This causes the upper and lower sidebands to become coherent and has been defined as conformability by Robbins [5]. The model is put in this form to highlight all the effects, which are often not clear in a block diagram model.

A general equation for the phase noise can be derived as shown in equation 1 [3] which allows for a number of operating conditions including power and the output and input impedances. F is the operating noise factor which includes the amplifier parameters under the oscillating operating conditions, k is the Boltzmann constant and T is the operating temperature. Q_0 is the unloaded Q, Q_L is the loaded Q, f_0 is the oscillator frequency and Δf is the offset frequency. P is the power in the oscillator which can be defined in two ways. P_{AVO} is the power available from the output of the amplifier and P_{RF} is the total power dissipated in the input, output, and equivalent loss resistances. N and A are integer variables which could be 1 or 2 dependent on the definition of P .

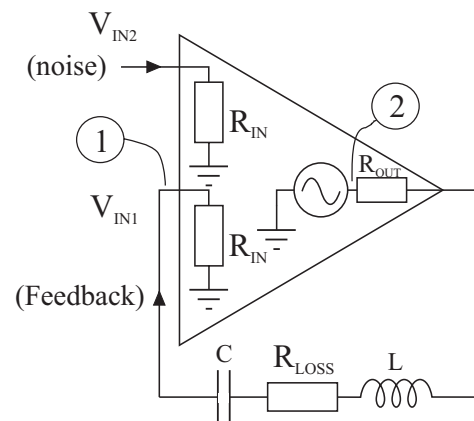


Figure 1 Oscillator Model

$$L(f) = A \cdot \frac{FkT}{8(Q_0)^2 (Q_L/Q_0)^2 (1 - Q_L/Q_0)^N P} \left(\frac{f_0}{\Delta f} \right)^2 \quad (1)$$

where:

1. $N = 1$ and $A = 1$ if P is defined as P_{RF} and $R_{OUT} = \text{zero}$.
2. $N = 1$ and $A = 2$ if P is defined as P_{RF} and $R_{OUT} = R_{IN}$.
3. $N = 2$ and $A = 1$ if P is defined as P_{AVO} and $R_{OUT} = R_{IN}$.

If we take expansion 3 and show the full equation including the impedances, we obtain equation 2 [3].

$$L(f) = \frac{FkT}{32Q_0^2 (Q_L/Q_0)^2 (1 - Q_L/Q_0)^2 P_{AVO}} \left(\frac{(R_{OUT} + R_{IN})^2}{R_{OUT} \cdot R_{IN}} \right) \left(\frac{f_0}{\Delta f} \right)^2 \quad (2)$$

The bracket including R_{OUT} and R_{IN} is minimum when $R_{OUT} = R_{IN}$ causing the whole bracket to equal 4. Equation 2 then simplifies to equation 3:

$$L(f) = \frac{FkT}{8Q_0^2 \left(\frac{Q_L}{Q_0} \right)^2 \left(1 - \frac{Q_L}{Q_0} \right)^2 P_{avo}} \left(\frac{f_0}{\Delta f} \right)^2 \quad (3)$$

This equation will be used in the analysis for the noise performance and gain requirements.

This equation has a further minimum when $Q_L/Q_0 = 1/2$ and hence when the insertion loss of the resonator is 0.25 (–6dB). This minimum occurs because the amplifier gain is set by the insertion loss of the resonator which is:

$$S_{21} = (1 - Q_L/Q_0) \quad (4)$$

This was first described by Parker in [2].

Under optimum conditions:

$$L(f) = \frac{2FkT}{Q_0^2 P_{AVO}} \left(\frac{f_0}{\Delta f} \right)^2 \quad (5)$$

Equation (5) is similar to Leeson's equation [1], although Leeson's equation used the loaded Q , Q_L , and the power incident on the input, P_I . Taking Leeson's Equation from [1] where the flicker noise parameters and the noise floor are left out, we obtain:

$$S_\phi(f) = \frac{FkT}{2Q_L^2 P_I} \left(\frac{f_0}{f} \right)^2 \quad (6)$$

where $S_\phi(f)$ is the spectral power density of phase fluctuations in radians squared per Hertz.

Taking the conditions that $P_I = P_{AVO}/4$ and $Q_L = Q_0/2$, based on the optima derived from equation (3), and assuming small angle modulation, then Leeson's equation becomes:

$$L(f) = \frac{S_\phi(f)}{2} = \frac{4FkT}{Q_0^2 P_{AVO}} \left(\frac{f_0}{f} \right)^2 \quad (7)$$

This version of Leeson's equation has the same form as equation (3) but is twice its value. This is because equation (3) incorporates the assumption that limiting causes the phase noise component to be half the total thermal noise. This lower noise floor is confirmed in [6] where they have shown 'theoretically and experimentally that the single sideband PM (and AM) noise floor due to thermal noise' (at room temperature) 'is -177dBc/Hz relative to a carrier input power of 0dBm'.

It should be noted that the noise factor, F , was assumed to be constant in this optimization. The noise factor may however vary with source impedance and hence Q_L/Q_0 as described in [7]. The noise factor may also show a power dependence which can be affected by both the device type and the amplifier topology. Examples of the effects of gain compression on the thermal (additive noise) and transposed flicker noise (modulation noise) are shown in [7]. If the inter-dependence is known then this can be incorporated to modify the optimum value of Q_L/Q_0 .

Based on equation 1, plots of noise degradation with Q_L/Q_0 are shown in Figure 2. This shows phase noise degradation for the two different definitions of power (P_{AVO} or P_{RF}). Also included are measurements on an oscillator in which the amplifier had a very low output impedance. [4]

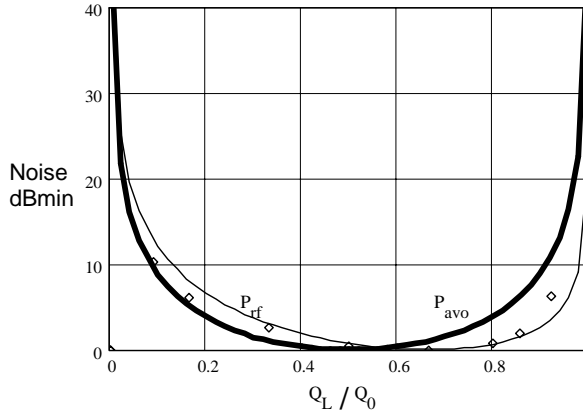


Figure 2 Phase Noise, dBmin vs Q_L/Q_0

To obtain further insight, a plot of noise degradation with resonator insertion loss and hence closed loop gain is shown in Figure 3. This gives a more obvious indication of the allowable tolerances on the insertion loss of a resonator. It can be seen that only one dB of noise degradation occurs when the insertion loss is within the bounds of 3.5 to 9.5dB.

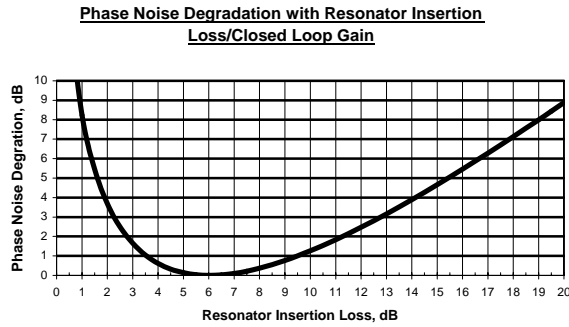


Figure 3, Phase noise degradation with resonator insertion loss/open loop gain

The requirements for minimum noise are therefore:

1. Q_0 is as high as possible
2. P_{AVO} is maximum and noise figure is minimum
3. $Q_L/Q_0 = 1/2$, therefore S_{21} of the resonator should be set to -6dB

It should be noted that the optima, just discussed, apply if the noise is thermal (additive) noise and also only apply to the skirts of the phase noise. For far out noise to be minimum the gain should be kept low (Q_L/Q_0 low) and for reduced transposed flicker noise the loaded Q should be higher. However this optimum is a good starting point.

Equation 3 can be extended to describe the phase noise including the effect of the noise floor, the transposed flicker noise and the noise contributions of the output couple and buffer amplifier. This is shown below in equation 8. The

right hand term is based on equation 3, the middle term shows noise outside the resonator bandwidth (far from carrier noise) and both these terms are multiplied by a flicker noise component $(1 + F_c/f)$. The left hand term includes the buffer amplifier after the output coupler and is still assumed to be limited by the phase noise measurement (therefore $2P$). The '1' refers to the phase noise of a single oscillator. This is changed to 2 when the combined noise of two identical oscillators is being displayed.

$$L(f) = 10 \log \left[1 + \left(\frac{F_c kT}{C_0 2P} + \left(1 + \frac{F_c}{f} \right) \left(\frac{F_c kT}{2P} \right) \left(\frac{1}{1 - \frac{Q_L}{Q_0}} \right) + \frac{F_c kT}{8(Q_0)^2 \left(\frac{Q_L}{Q_0} \right)^2 \left(1 - \frac{Q_L}{Q_0} \right)^2 P} \left(\frac{f_0}{f} \right)^2 \right) \right] \quad (8)$$

III. OSCILLATOR CONFIGURATION

A typical block diagram of a narrow tuning oscillator using phase shift tuning is illustrated in Figure 4. This consists of an amplifier, output coupler, filter to ensure operation at the correct resonant frequency, the resonator and in this case a voltage controlled phase shifter for narrow band tuning.

It should also be noted that for accurate analysis and noise prediction, all the items other than the resonator should be combined into an 'equivalent amplifier block' and the required Noise Figure, open loop gain and P_{AVS} should be calculated and/or measured. We have found, using these techniques, that the noise predictions are almost always within 0 to 2dB of the theory.

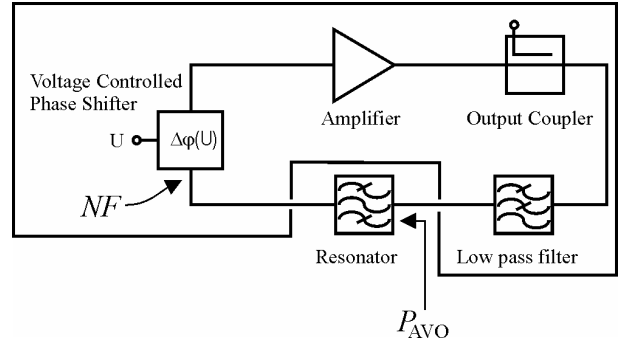


Figure 4 Block Diagram used for calculation of phase noise using Noise Factor (NF), P_{AVO}

To achieve best performance each element should be designed and optimized separately. The major parameters for the loop amplifiers, resonators and tuning elements will now be described.

A. AMPLIFIERS

The amplifiers should offer:

1. Well defined input and output impedance
2. Low noise figure
3. Low Residual Flicker Noise using optimum bias. Flicker noise corners $< 5\text{kHz}$ should be achievable at RF and microwave frequencies and $< 20\text{Hz}$ at low frequencies
4. Low dependence on power supply noise and low regulator noise
5. Well defined limited output power
6. Smooth monotonic saturation characteristics with negligible change in parameters
7. Unconditional stability both in the linear and saturation regions

All of these parameters are interdependent and therefore need to be optimised carefully.

B. Resonators

Resonators should offer:

1. High unloaded Q . It is important to ensure uniform current distribution in metal surfaces and this is usually improved with symmetry.
2. Low and where possible far removed spurious responses. If required additional filters can be incorporated to ensure sufficient loss at the unwanted resonance.
3. Correct coupling: Design the coupling network to achieve an insertion loss of 6dB. Note that only 1dB noise degradation occurs if the insertion loss is within the bounds of -3.5 to -9.5dB.
4. Low sensitivity to external parameters such as temperature and vibration

These techniques have been applied successfully to LC (inductor capacitor), transmission line (printed and ceramic), crystal, SAW and Dielectric resonators.

C. TUNING ELEMENTS

1) Phase Shifter Method

Frequency tuning is typically achieved by incorporating the varactor diodes either into the resonator or by using phase shift tuning separate from the resonator as illustrated in Figure 4. Phase shift tuning has the advantage that it does not degrade the resonator unloaded Q and the phase noise degradation can be accurately calculated. This group has

shown (theoretically and experimentally) that the noise performance degrades with a $\cos^4\theta$ relationship [3] [7]. Therefore an open loop phase error of 45° causes 6dB degradation + the insertion loss of the phase shifter. This is illustrated in figure 5.

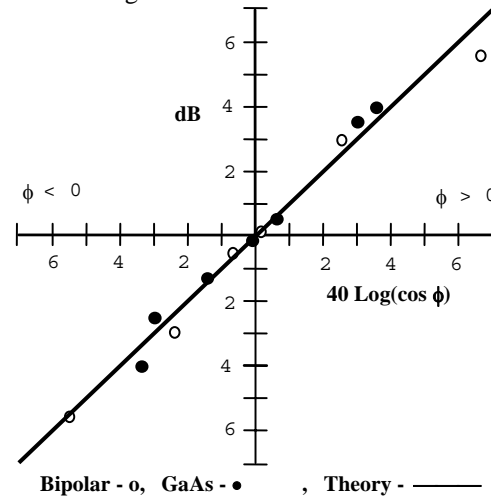


Figure 5 Phase noise degradation with open loop phase error

The phase shifter should have low insertion loss and a near linear phase vs frequency response. It is important to ensure that the change in insertion loss and phase shift does not change significantly with power level. In fact this is even more critical in varactor tuned resonators where the Q is higher.

2) Varactor controlled resonator method

The noise performance of a broad tuning range oscillator is usually limited by the Q and the voltage handling capability of the varactor as has been described by Underhill [8]. These equations were extended to include oscillators operating under optimum conditions [3], [9], and are described here for general conditions which relate this operating AC voltage to the coupling coefficient and hence Q_1/Q_0 . This is examined by taking a simple model for the resonator as shown in Figure 6. This consists of a series LCR network which can be used to model both series and parallel resonators. All the losses from the varactor, inductor and capacitor are combined into R_{LOSS} .

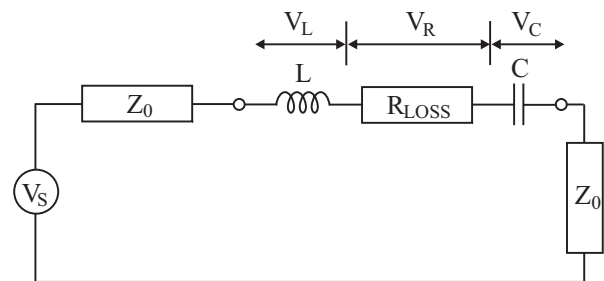


Fig. 6. General Model for Resonator

The power dissipated in the resonator loss resistance, R_{LOSS} , is:

$$P_{RES} = \frac{V_R^2}{R_{LOSS}} \quad (9)$$

The voltage across the capacitor V_C in a resonator is:

$$V_C = Q_0 V_R \quad (10)$$

Therefore the power dissipated in the resonator is now:

$$P_{RES} = \frac{V_C^2}{Q_0^2 R_{LOSS}} \quad (11)$$

The power dissipated in the resonator can be calculated in terms of P_{AVO} and Q_L/Q_0 by using:

$$P_{avo} = \frac{V_s^2}{4Z_0} \quad (12)$$

So From Figure 6:

$$Q_L = \frac{\omega L}{R_{LOSS} + 2Z_0} \quad (13)$$

$$Q_0 = \frac{\omega L}{R} \quad (14)$$

$$\therefore \frac{Q_L}{Q_0} = \frac{R_{LOSS}}{R_{LOSS} + 2Z_0} \quad (15)$$

$$V_R = V_s \cdot \frac{R}{R_{LOSS} + 2Z_0} = \left(\frac{Q_L}{Q_0} \right) \cdot V_s \quad (16)$$

From (9), (12), (15) and (16)

$$\therefore P_{RES} = 2 \frac{Q_L}{Q_0} \cdot \left(1 - \frac{Q_L}{Q_0} \right) \cdot P_{AVO} \quad (17)$$

When $Q_L/Q_0 = 1/2$, $P_{RES} = P_{AVO}/2$. If it is assumed that the varactor losses are dominant then the noise performance is set totally by the varactor loss resistance and the voltage handling capability to be [3] [8]:

$$L(f) = \frac{FkTR_{LOSS}}{V_C^2} \left(\frac{f_0}{\Delta f} \right)^2 \quad (18)$$

Note that if a parallel resonator is used then this series model can still be used by converting the parallel loss resistances R_p to series loss resistances R_s . For reasonable values of Q :

$$Q_0 = \frac{\omega L}{R_s} = \frac{R_p}{\omega L} \quad (19)$$

Therefore:

$$R_s = \frac{(\omega L)^2}{R_p} \quad (20)$$

It is interesting to note that non linear effects occur at surprisingly low power levels as illustrated in Figure 7. This consists of an LC resonator with a loaded Q of 63 with 3 volts DC bias on the varactors. Distortion starts to occur at -6dBm!

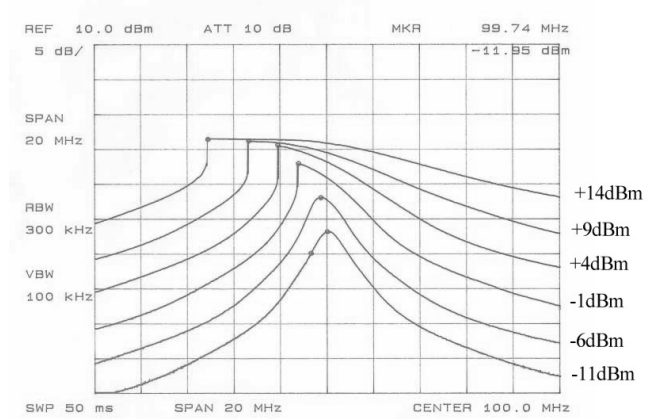


Figure 7. Distortion effects in varactor tuned resonators vs power available at the input

IV. OSCILLATOR DESIGN AND LABORATORY

It is interesting to apply the design rules developed so far to the LC feedback oscillator shown in Figure 8. This is offered as a 3 hour laboratory class to our 4th year MEng and Masters students as part of the RF and Microwave Circuit Design Course. This course is also offered to industrial students and companies both on and off site. The book for this course is reference [3]. The students are asked to design a 100MHz LC oscillator.

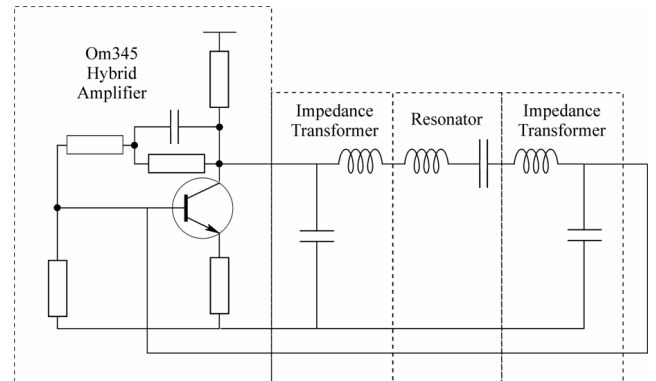


Figure 8, LC Oscillator circuit

The students are required to theoretically design the resonator to obtain $Q_L/Q_0 = 1/2$. Initially they measure the unloaded Q of the resonator. They adjust the theoretical response of the resonator for the effects of parasitics through simulation and then build and measure the complete resonator. They then close the loop and measure the phase noise of the oscillator using the phase detector method. The whole design is achieved on a single printed circuit board as illustrated later.

The impedance networks are designed to obtain the correct $Q_L/Q_0 = 1/2$. This full calculation procedure is described in [3] and [9] and summarized here. Note that the inductors in the resonator merge to form a single inductor at the end of the design.

The unloaded Q of the resonator should be known or can be measured using the two loop technique described in [3][9]. These loops are connected to a network analyzer and S_{21} is measured

Two loops are overlaid to obtain low coupling at the operating frequency as shown in Figure 9.

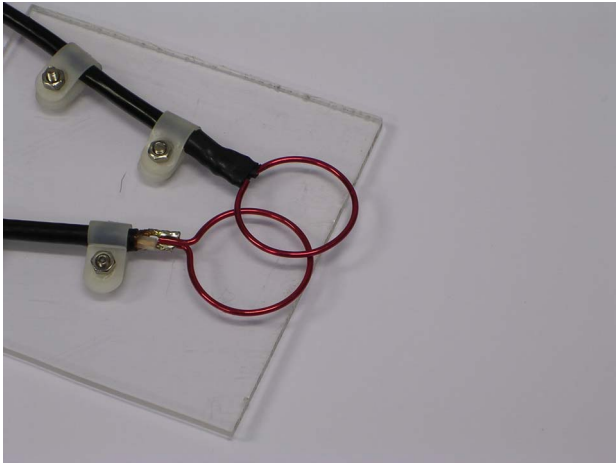


Figure 9. Overlaid loops adjusted for minimum coupling

The coil is then resonated with a trimmer capacitor and loosely coupled to the centre of the loops as illustrated in Figure 10. The coil/capacitor is mounted in a cut-down inverted plastic cup. By ensuring the insertion loss is greater than 20dB the unloaded Q can be obtained from the 3dB points.

The resonator is then designed using the following procedure.

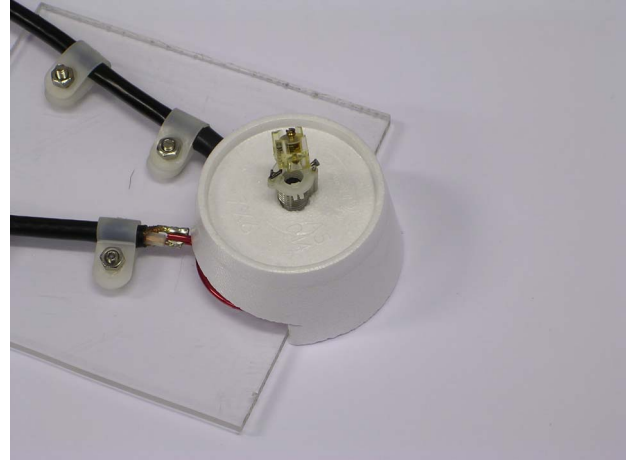


Figure 10. Overlaid loops adjusted for minimum coupling

A. Resonator Design

1. Model the resonator as a series LCR circuit as shown in Fig. 11.



Figure 11, LCR resonator

2. Merge all the loss resistances of the varactor and the inductor and capacitor into R_{LOSS} .
3. Set $S_{21} = -6$ dB ($Q_L/Q_0 = 1/2$) by making the source resistance seen by the resonator, $Z_0 = R_{LOSS}/2$ as shown in Fig. 12.

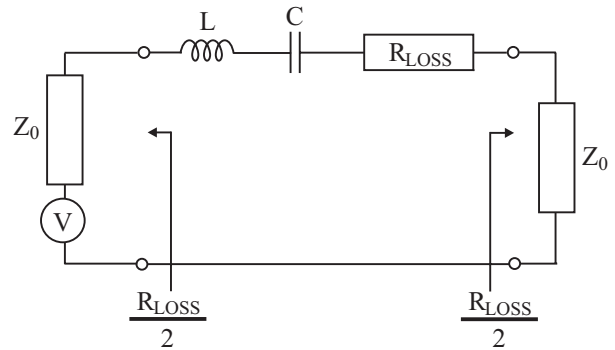


Figure 12, Make source resistance = R_{LOSS}

4. Design LC impedance transformation networks to achieve item 3 above as shown in Fig. 13. As the total inductance required is L, subtract $2L'$ from L and calculate the value of C for the resonant frequency.
5. Now incorporate $2L'$ into L to make the total value L

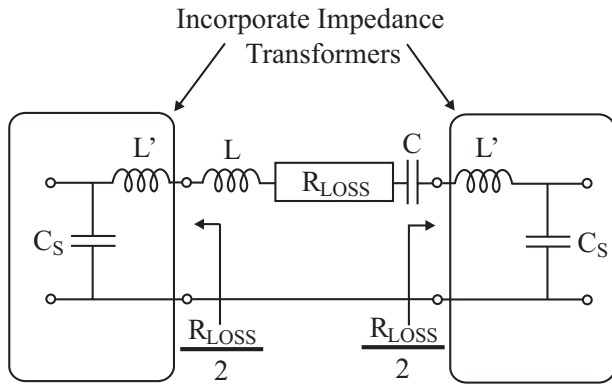


Fig. 13. Resonators with impedance transformers.

The final circuit is shown in Fig. 14.

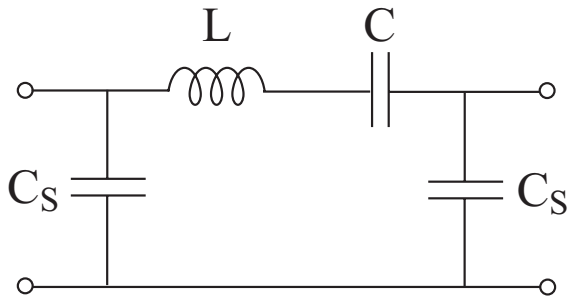


Figure 14, Final Resonator

It should be noted that the value of C_S is often rather large and that parasitic inductances often increase the equivalent capacitor value. In a simulation a parasitic inductance is added and the effect is illustrated in Figure 15 for a resonator operating at 150MHz. The ideal response is in the centre of the picture and the effect of adding 1nH and then 2nH of parasitic inductance in series with C_S is shown. By reducing C_S the original response can be re-obtained.

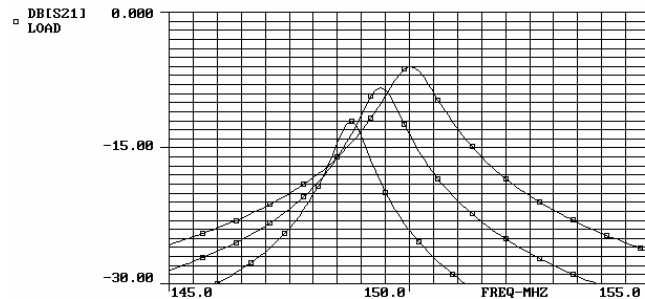


Figure 15. Effect of parasitic inductance in C_S

The students are provided with a printed circuit board (Figure 16) which contains a broadband amplifier (based on a design taught elsewhere in the course [3]). This printed circuit board enables the resonator to be built and tested separately. Once tested on a network analyzer to achieve $S_{21} \sim -6\text{dB}$ the oscillator loop is closed and the phase noise measured.

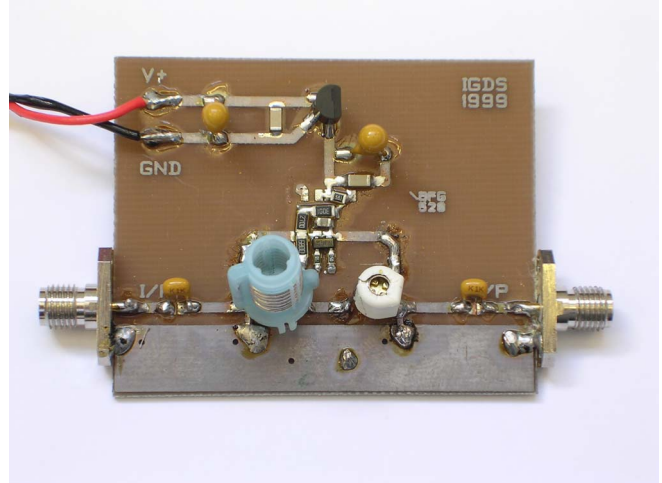


Figure 16, LC Oscillator board for open and closed loop measurement

The students are also offered another design which uses a printed transmission line resonator which operates at 1GHz.

Note it is also possible to implement tuning by inserting a varactor diode and incorporating the DC bias by adding low value resistors at the low impedance points that are at the input and output as shown in Fig. 17. These resistors should be $> 50 \Omega$ to avoid loading the 50Ω terminating impedances but still fairly low to ensure that they do not degrade the noise performance of the oscillator [3]. Inductors could be used, but resistors are less likely to cause unwanted resonances. Note that the loss resistances for the varactor are included in the calculations from the beginning (causing lower Qs) but the phase noise is still accurately predicted.

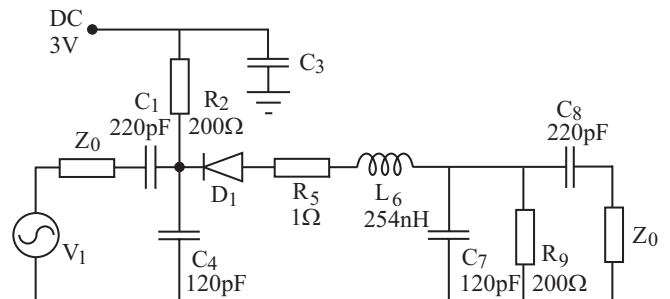


Figure 17, Simple Varactor Tune LC resonator

A variety of resonator and oscillator designs are described in [3], [10-18] including both narrow and broad band tuning and high Q printed and ceramic resonators. A table of the current performance achieved is illustrated in Table 1.

Table 1 Phase noise performance of oscillators vs frequency

| Freq GHz | Osc Type | Phase Noise 10kHz, dBc/Hz | Noise Floor dBc/Hz | Electronic Tuning | Modulation Bandwidth |
|----------|--------------|---------------------------|--------------------|-------------------|----------------------|
| 10MHz | Crystal | -118, 1Hz -147, 10Hz | < -160 | Few Hz | |
| 1.25 | DRO | -170 | < -180 | Yes | |
| 1.5 | CRO | -127 | < -165 | 3MHz | >2MHz |
| 4 | DRO | -152 | < -170 | 250kHz | >200kHz |
| 8 | DRO flatpack | -123 | < -170 | Yes | |
| 10 | DRO | -135 | < -170 | 300kHz | >200kHz |

V. ACKNOWLEDGEMENTS

I wish to thank the UK Engineering and Physical Sciences Research Council for supporting this work. I would also like to thank Simon Bale, Jens Bitterling, Carl Broomfield, Michael Cheng, Frazer Curley, Paul Dallas, Mike Page-Jones, Marc Sallin, Richard Thomas, Konstantinos Theodouropoulos, Yiming You and Liang Zhou for their help in generating new ideas and results.

VI. CONCLUSIONS

A simple and accurate linear theory for oscillator design has been described. A set of design rules has been developed and a detailed design example has been described.

VII. REFERENCES

- [1] D.B. Leeson, "A Simple Model of Feedback Oscillator Noise Spectrum", Proceedings of the IEEE, 54, pp. 329-330, Feb. 1966.
- [2] T.E. Parker, "Current Developments in SAW Oscillator Stability", Proceedings of the 31st Annual Symposium on Frequency Control, Atlantic City, New Jersey, 1977, pp. 359-364.
- [3] Jeremy Everard, "Fundamentals of RF Circuit Design with Low Noise Oscillators", ISBN: 0-471-49793-2, Wiley, Dec. 2000 reprinted Oct. 2002.
- [4] Jeremy Everard, "Low Noise Power Efficient Oscillators: Theory and Design," Proceeding of the IEE, pt G, 133, No.4, pp172-180, 1986.
- [5] W.P. Robins, "Phase Noise in Signal Sources," IEE, Peter Perigrinus, 1992.
- [6] A. Hati, D. A. Howe, F. L. Walls, and D. Walker, "Noise figure vs PM noise measurements: A study at microwave frequencies," Proc. IEEE Int. Freq. Contr. Symp. Digest, 2003, pp. 516-520.
- [7] K.K.M. Cheng and J.K.A. Everard, "Noise Performance Degradation in Feedback Oscillators with non zero Phase Error". Microwave and Optical Technology Letters, 4, No. 2, pp. 64 - 66, 1991.
- [8] M.J. Underhill, "Oscillator Noise Limitations", IERE Conference Proceedings 39, pp.109-118, 1979.
- [9] 28. J.K.A. Everard and L. Zhou. "Non Linear Effects in varactor tuned resonators" IEEE Transactions on Ultrasonics Ferroelectrics and Frequency Control, Vol. 53, No. 5, May 2006, pp.853 - 861.
- [10] J.K.A. Everard and C. Broomfield, "Reduced Transposed Flicker Noise in Microwave Oscillators using GaAs based Feedforward Amplifiers and Low Frequency Feedback", IEEE Transactions on Ultrasonics Ferroelectrics and Frequency Control. Vol. 54, No. 6, June 2007, pp.1108 - 1117.
- [11] J.K.A. Everard and Keng Ng 'Ultra-Low Noise Crystal Oscillators' TimeNav2007, Geneva.
- [12] Jeremy K.A. Everard and Konstantinos Theodoropoulos 'Ultra-Low Phase Noise Ceramic based Dielectric Resonator Oscillators', IEEE Frequency Control Symposium, Miami USA, June 2006.
- [13] J.K.A. Everard and C Broomfield, High Q printed Helical Resonators for Low Noise Oscillators and Filters", to be published IEEE Transactions on Ultrasonics Ferroelectrics and Frequency Control
- [14] Carl Broomfield, Yiming You, Richard Parsons and Jeremy Everard, 'Broad Tuning Microwave Oscillators Utilising Multilayer Technology and Sige Devices', Proceedings of the 2003 IEEE International Frequency Control Symposium held jointly with the European Frequency and Time Forum, Tampa USA, May 2003, pp. 417 - 422.
- [15] J.K.A. Everard and K.K.M. Cheng. "Novel Low noise 'Fabry Perot' transmission line oscillator". IEE Electronics Letters, 17th August 1989, Issue 17, Vol. 25, pp.1106-1108.
- [16] K.K.M. Cheng and J.K.A. Everard. "Novel varactor tuned transmission line resonator". IEE Electronics Letters, 17th August 1989, Issue 17, Vol. 25, pp.1164-1165.
- [17] K.K.M. Cheng and J.K.A. Everard "X band Monolithic Tunable Resonator/Filter". IEE Electronics Letters, 9th November 1989, Vol.25, No.23, pp.1587-1589.
- [18] J.K.A. Everard, K.K.M. Cheng and P.A. Dallas. "A High Q Helical Resonator for Oscillators and Filters in Mobile Communications Systems" IEE Electronics Letters, 23rd November 1989, Vol. 25, No.24, pp. 1648-1650.